

## Nonpeptidic, Monocharged, Cell Permeable Ligands for the p56lck SH2 Domain

John R. Proudfoot,\* Rajashehar Betageri, Mario Cardozo, Thomas A. Gilmore, Susan Glynn, Eugene R. Hickey, Scott Jakes, Alisa Kabcenell, Thomas M. Kirrane, Annette K. Tibolla, Susan Lukas, Usha R. Patel, Rajiv Sharma, Mehran Yazdanian, and Neil Moss

Boehringer Ingelheim Pharmaceuticals Inc., 900 Ridgebury Road, P.O. Box 368, Ridgefield, Connecticut 06877

Pierre L. Beaulieu, Dale R. Cameron, Jean-Marie Ferland, Jean Gauthier, James Gillard, Vida Gorys, Martin Poirier, Jean Rancourt, Dominik Wernic, and Montse Llinas-Brunet

Boehringer Ingelheim (Canada) Ltd., Research and Development, 2100 Cunard Street, Laval, Quebec H7S 2G5, Canada

Received October 16, 2000

p56lck is a member of the src family of tyrosine kinases and plays a critical role in the signal transduction events that lead to T cell activation. Ligands for the p56lck SH2 domain have the potential to disrupt the interaction of p56lck with its substrates and derail the signaling cascade that leads to the production of cytokines such as interleukin-2. Starting from the quintuply charged (at physiological pH) phosphorylated tetrapeptide, AcpYEELI, we recently disclosed (*J. Med. Chem.* **1999**, *42*, 722 and *J. Med. Chem.* **1999**, *42*, 1757) the design of the modified dipeptide **3**, which carries just two charges at physiological pH. Here we present the elaboration of **3** to the nonpeptidic, monocharged compound, **9S**. This molecule displays good binding affinity for the p56lck SH2 domain ( $K_d$  1  $\mu$ M) and good cell permeation, and this combination of properties allowed us to demonstrate clear-cut inhibitory effects on a very early event in T cell activation, namely calcium mobilization.

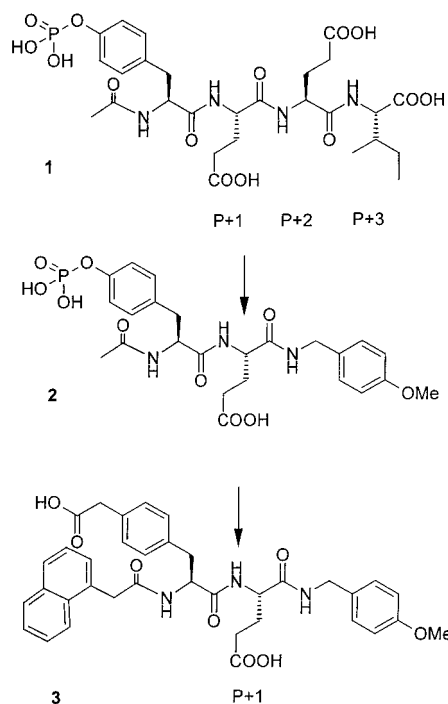
### Introduction

Src homology-2 (SH2) domains are protein modules of about 100 amino acids that bind to phosphotyrosine-containing peptide sequences. These domains function as regulatory elements in cell signaling processes by controlling the activity and localization of tyrosine kinases and other proteins involved in signal transduction.<sup>1</sup> They are attractive targets for drug discovery efforts, especially in the areas of oncology and immunology, and several reports have appeared recently on the design of ligands for the SH2 domains of pp60c-src,<sup>2–4</sup> Grb2,<sup>5,6</sup> and p56lck.<sup>7</sup>

The lead structures for these efforts are usually phosphotyrosine-containing peptides, and most of the reported ligands are at least doubly charged at physiological pH and often retain some peptidic character. These two features are considered impediments to cell permeation, and, although ligands with good binding affinity to various SH2 domains are available, prodrug<sup>3c,8</sup> and more exotic approaches<sup>9</sup> have generally been needed to deliver these ligands into cells.<sup>10</sup> Recently, cellular activity that does not rely on these approaches has been reported for a monocharged ligand of the src SH2 domain.<sup>11</sup>

Our interest in interfering with the function of p56lck,<sup>12</sup> a tyrosine kinase that plays a critical role in T cell activation, led us to design ligands for the SH2 domain of p56lck.<sup>13</sup> Such ligands have the potential to block the interaction of p56lck with its substrates such

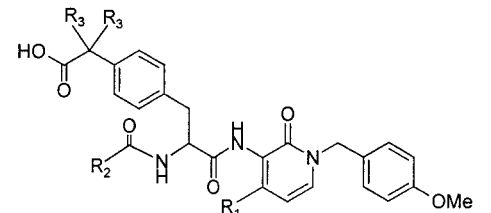
### Scheme 1

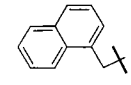
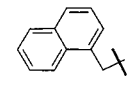
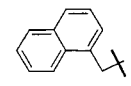
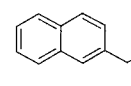
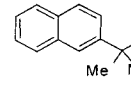
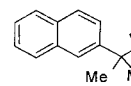
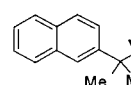


as the T cell receptor and the tyrosine kinase ZAP70. This could derail the signaling cascade that in CD4<sup>+</sup> T cells leads to the production of cytokines such as interleukin-2 (IL-2), and, ultimately, to cell proliferation. The ligands could therefore provide a novel means to control the immune response.

The peptide **1**, AcpYEELI,<sup>14</sup> (Scheme 1) which binds to the p56lck SH2 domain with high affinity ( $K_d$  = 0.1  $\mu$ M), served as the starting point for our efforts.<sup>15,16</sup> Our

\* Address correspondence to John R. Proudfoot at Department of Medicinal Chemistry, Boehringer Ingelheim Pharmaceuticals Inc., 900 Ridgebury Road, PO Box 368, Ridgefield CT 06877. Phone: (203) 798 5107. Fax: (203) 791 6072. E-mail: jproudf@rdg.boehringer-ingelheim.com.

Table 1<sup>a</sup>


Compound	R <sub>1</sub>	R <sub>2</sub>	R <sub>3</sub>	K <sub>d</sub> (μM) <sup>a</sup>	P <sub>caco-2</sub> 10 <sup>6</sup> (cm/sec)	% Permeated in 3 hours
3				5 μM	0.04 +/- 0.07 (A→B) 0.19 +/- 0.07 (B→A)	0.3
4	H		H	23 +/- 9 (4)	0.45 +/- 0.02 (A→B)	1.3
5	CH <sub>3</sub>		H	1.3 +/- 0.5 (4)	0.08 +/- 0.01 (A→B) 10.9 +/- 0.5 (B→A)	0.3
6	CH <sub>3</sub>	CH <sub>3</sub>	H	7 +/- 2 (4)	0.1 +/- 0.1 (A→B)	0.4
7RS	CH <sub>3</sub>		CH <sub>3</sub>	1.2 +/- 0.7 (7)	0.15 +/- 0.02 (A→B) 22.4 +/- 0.9 (B→A)	0.4
8RS	CH <sub>3</sub>		CH <sub>3</sub>	0.28 +/- 0.09 (6)	0.19 +/- 0.02 (A→B) 23.0 +/- 0.5 (B→A)	0.6
9RS	CH <sub>3</sub>		CH <sub>3</sub>	1.2 +/- 0.4 (6)	6.1 +/- 0.2 (A→B)	17
9R	CH <sub>3</sub>		CH <sub>3</sub>	50 +/- 30 (4)	6.8 +/- 0.4 (A→B)	16
9S	CH <sub>3</sub>		CH <sub>3</sub>	1 +/- 0.2 (4)	7.7 +/- 0.7 (A→B) 38.9 +/- 0.7 (B→A)	21

<sup>a</sup> Number of determinations in brackets.

goal was the transformation of this molecule into a cell permeable ligand with demonstrable efficacy in cellular models of T cell activation. We viewed the five negative charges at physiological pH, the metabolically unstable phosphate group, and the peptidic nature of **1** as undesirable characteristics. We previously described the studies that led us to peptide **2** in which the two C-terminal amino acids were replaced with a *p*-methoxybenzyl group.<sup>7a</sup> Peptide **2**, with two fewer carboxyl groups, has affinity equal to **1** for the p56lck SH2 domain. Concurrent efforts to find a metabolically stable, less charged, alternative for the phosphate group gave us structure **3**, which contains an acetic acid group as a phosphate replacement.<sup>7b</sup> Replacement of the doubly charged phosphate group with the singly charged acetic acid group results in decreased binding affinity of between 200- and 500-fold for the SH2 domain.<sup>7b,17</sup> However, binding affinity is partly recovered, to the extent of about 10-fold, with the introduction of lipophilic substituents, particularly naphthylacetyl groups as shown, at the N terminus,<sup>7b</sup> a beneficial effect also noted by others working this area.<sup>18</sup> At this point we had transformed the tetrapptide **1** with five negative charges at physiological pH into the dipeptide **3** with

two negative charges, albeit at the cost of a 50-fold decrease in binding affinity. In addition, compound **3** is very poorly cell permeable (Table 1), and we expected that substantial improvement in binding affinity and/or permeability would be required before efficacy in cellular assays could be demonstrated.

Our driving hypothesis was that a monocharged ligand should provide the best balance between affinity for the SH2 domain and physical properties that would allow cell permeability and the demonstration of cellular activity. Here we describe the continuation of our efforts, and the elaboration of **3** to a cell permeable molecule, with low micromolar binding affinity for the p56lck SH2 domain, and demonstrable cellular efficacy.

### Design of an Effective Backbone Modification

The progress described in our previous two manuscripts, and outlined above, came from changes at the N- and C-termini of the peptide **1** (Scheme 1). Our early attempts to modify the P+1 region and dispense with the carboxylate-containing P+1 side chain met with mixed results. In the crystal structure of compound **1** bound to the p56lck SH2 domain, the P+1 carboxylic acid containing side chain does not interact directly with

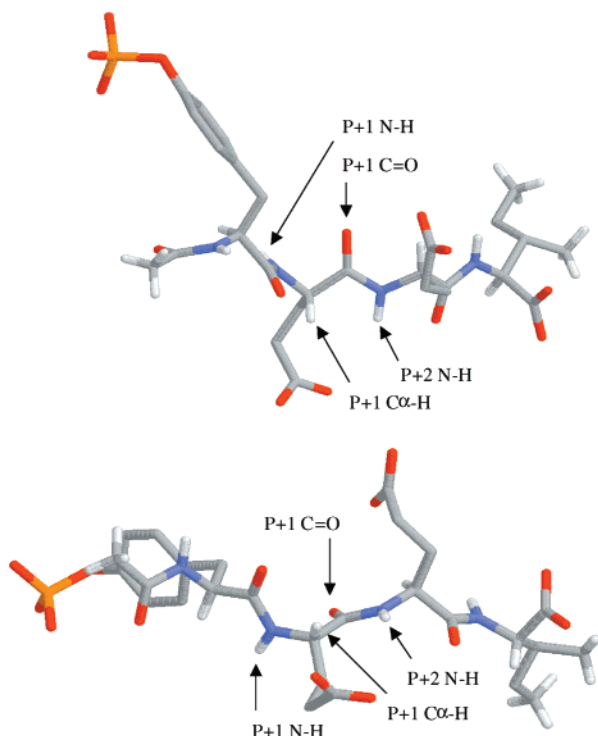


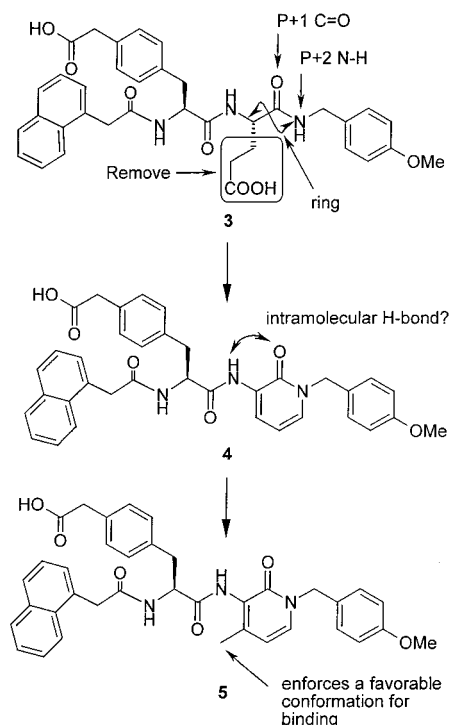
**Figure 1.** Two depictions of the bound conformation of **1**.

the protein.<sup>15</sup> SAR studies showed that it could be replaced by uncharged side chains without great cost to binding affinity, if done in the context of tetrapeptides<sup>19</sup> and pentapeptides.<sup>2a</sup> However, in the context of molecules such as **2**, we observed that incorporation of an uncharged side chain (leucine being the best) led to a 10-fold decrease in binding affinity.<sup>7a</sup> As we had already lost binding affinity due to the phosphotyrosine replacement, we felt that, in order to be successful, we needed to identify a noncharged replacement for the P+1 glutamic acid side chain that at least did not lose binding affinity.

In the bound conformation of **1** we noted that the C $\alpha$ -H of P+1 and the N-H of P+2 (indicated in Figure 1) are almost coplanar and point in the same direction. Our earlier SAR studies had shown that methylation is tolerated at the P+2 nitrogen atom in analogues of **1**,<sup>19</sup> and similar N-methylation is also tolerated in compounds related to **2**.<sup>7a</sup> The binding conformation of **1** depicted in Figure 1, and the tolerance of N-methylation at P+2 prompted various cyclization strategies directed toward rigidifying this region of the molecule.

Our most successful modification is illustrated in structure **4**, (Scheme 2). The P+1 side chain of **3** is discarded, and the P+1 carbonyl group and the P+2 nitrogen atom are incorporated into a pyridone ring,<sup>20</sup> attached to the P+1 C $\alpha$ . This modification was particularly attractive since the charged side chain is eliminated. Additionally, only one chiral center remains in the proposed molecule. We hoped that the loss in binding affinity due to the lack of a P+1 side chain would be recovered by the rigidification of the molecule. The conformational properties around the pyridone moiety of **4** suggested that one additional structural modification would be necessary. In structure **4**, the P+1 NH can participate in a favorable electrostatic interaction with the carbonyl group of the pyridone ring. This

## Scheme 2

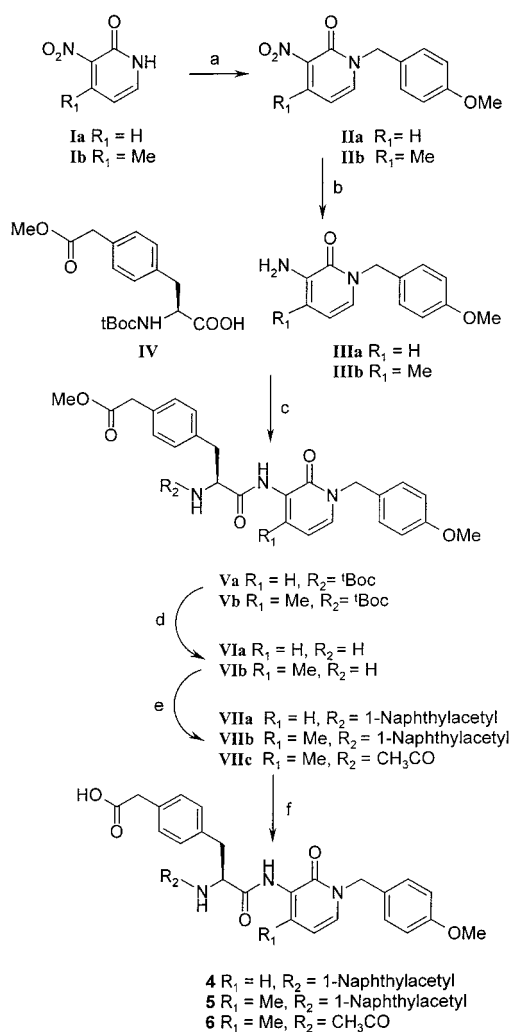


favors a planar disposition of the pyridone and the adjacent amide, which was predicted to be detrimental for binding to the SH2 domain. For example, in the structure of peptide **1** bound to the SH2 domain, the P+1 N-H is almost orthogonal to the P+1 carbonyl group (Figure 1) and partakes in an important hydrogen-bonding interaction with the SH2 domain. Introduction of a methyl substituent at the 4-position of the pyridone ring, as in structure **5**, ensures that the P+1 NH is orthogonal to the plane of the ring and available for a hydrogen-bonding interaction with the protein.

These conformational preferences for **4** and **5** were confirmed by ab initio quantum mechanics calculations. For compound **4**, calculations in a vacuum using Gaussian HF/6-31G\* basis set showed that the coplanar conformation of the amide and pyridone ring is preferred by about 5 kcal/mol over the orthogonal arrangement. This conformation possesses the intramolecular hydrogen bond between the NH of amide and the carbonyl group of the pyridone. In addition, the effect of solvent was taken into account by computing the solvation free energy for all rotamers. This thermodynamic quantity was estimated using a continuum self-consistent reaction field method (SCRF).<sup>21,22</sup> Thus, when the effect of solvent is taken into account, this planar conformation remains the most stable by 3 kcal/mol. For compound **5**, with the 4-methyl substituent, there is a calculated energy minimum in a vacuum at about 65°, and the 90° conformer is less favored by only about 1 kcal/mol. Calculations indicate that for **5** the solvent effect stabilizes the 90° conformer by about 1 kcal/mol relative to vacuum, indicating that the binding conformer should be favored in solution.

## Synthesis and Results

The synthesis of the target ligands is outlined in Scheme 3. The aminopyridinones **IIIa** and **IIIb**, precur-

Scheme 3<sup>a</sup>

<sup>a</sup> Conditions: (a) NaH, DMF, *p*-methoxybenzyl chloride; (b) H<sub>2</sub>, 10% Pd/C, ethanol; (c) EDC, CH<sub>2</sub>Cl<sub>2</sub>; (d) TFA, CH<sub>2</sub>Cl<sub>2</sub>; (e) naphthylacetic acid, EDC, CH<sub>2</sub>Cl<sub>2</sub> or acetic anhydride, CH<sub>2</sub>Cl<sub>2</sub>; (f) NaOH, THF, methanol, or LiOH, THF, H<sub>2</sub>O.

sors to the right-hand side of the targets, are derived in a straightforward manner from 3-nitro-2-pyridone and 4-methyl-3-nitro-2-pyridone, respectively, via *N*-alkylation followed by reduction of the nitro group as shown. The amino acid derivative **IV**<sup>7b,23</sup> is coupled with the amine **IIIa** or **IIIb** using standard conditions to give the amide **Va** or **Vb** in good yield. Unblocking of the *N*-terminus, followed by *N*-acylation and hydrolysis of the methyl ester, all proceed under standard conditions to give the compounds **4–6**.

Compound **5** binds to the SH2 domain with a *K*<sub>d</sub> of 1.3 μM (Table 1), i.e., it is 3-fold more potent than the analogous compound **3** containing a glutamic acid residue at P+1. This was an encouraging result. We had finally dispensed with the charged side chain and even improved binding affinity slightly in the process. Compound **6**, with an acetyl substituent at the *N*-terminus, shows a decrease in binding affinity (*K*<sub>d</sub> = 7 μM) consistent with that seen for *N*-acetyl vs *N*-naphthylacetyl comparisons in earlier series. This result gave us some confidence that these molecules were binding in an analogous manner to our earlier structures. The ligand lacking the methyl group at the 4-position of the pyridone ring, compound **4**, is considerably weaker (*K*<sub>d</sub>=

23 μM) than analogue **5**, thus supporting the conformational arguments used in the design of the pyridones.

Although we do not have crystal structures of our ligands bound to the SH2 domain, we have generated a model<sup>24</sup> that illustrates what we believe to be the important features involved in binding. In the model, depicted in Figure 2, the *p*-methoxybenzyl group is oriented toward the P+3 hydrophobic pocket. The phenyl ring is perpendicular to the plane of Tyr181, in position for a favorable edge-to-face aromatic–aromatic interaction. The methoxy substituent is located deep in the lipophilic pocket, with the methyl group in van der Waals contact with Leu216, Ile193, and Ser194. The pyridone ring lies on the surface of the protein, above tyrosine 181, while the NH of the “out-of-plane” amide group participates in a hydrogen bond with the backbone carbonyl of His180. The acetic acid group binds in the phosphate recognition pocket, as previously described.<sup>7b</sup> Figure 3 depicts an overlap of this model with the crystal structure of the complex between the p56lck SH2 domain and Ac-pTyr-Glu-Glu-Ile (ligand shown in purple).

Although compound **5** represents a significant advance over compound **3**, it still showed apparently poor cell permeation properties when evaluated in a Caco-2 model<sup>25</sup> of cell permeability (Table 1). Despite the possibility that the apparent poor permeation of **5** could in part be rationalized by an efflux mechanism, we concentrated on identifying groups that might be expected to improve cell permeability (i.e., enhance desolvation). In general, the diffusion of molecules across cell membranes is enabled by the shielding or elimination of hydrogen-bonding functionality.<sup>26,27</sup> With regard to structure **5**, options for eliminating hydrogen-bonding capacity were somewhat limited. Methylation of either remaining amide nitrogen decreases binding affinity by at least 10-fold,<sup>19</sup> and we preferred avoiding a prodrug approach with respect to the carboxylic acid. Since we knew from our earlier SAR studies that small lipophilic substituents are tolerated adjacent to the carboxylate group,<sup>19</sup> we targeted the α,α-dimethyl derivative **7**, expecting the methyl substituents to shield the polar carboxylate functionality and enhance the cell permeation properties relative to **5**. Since both the 1- and 2-naphthylacetyl *N*-terminus substitution had been effective in earlier series, analogue **8** was also synthesized.

The synthesis of compounds **7** and **8** is outlined in Scheme 4. The dimethylacetic acid intermediate **X** was synthesized in racemic form. It was derived in a straightforward manner from a Heck reaction of *N*-Boc-dehydroalanine benzyl ester<sup>28</sup> with the iodophenylacetic acid derivative **VIIIc**, followed by catalytic hydrogenation to saturate the double bond and remove the benzyl group. The only other difference of note from the methods described in Scheme 3 is the use of the *tert*-butyl ester as a protecting group for the carboxylic acid. Initially, selective removal of the *N*-Boc group presented some difficulty, but we eventually found that HCl in dioxane was effective in removing the Boc group while leaving the ester intact.

The effects of dimethyl substitution adjacent to the carboxylate group and the P-1 amide are illustrated in Table 1. The comparison of dimethyl derivative **7RS** (*K*<sub>d</sub>

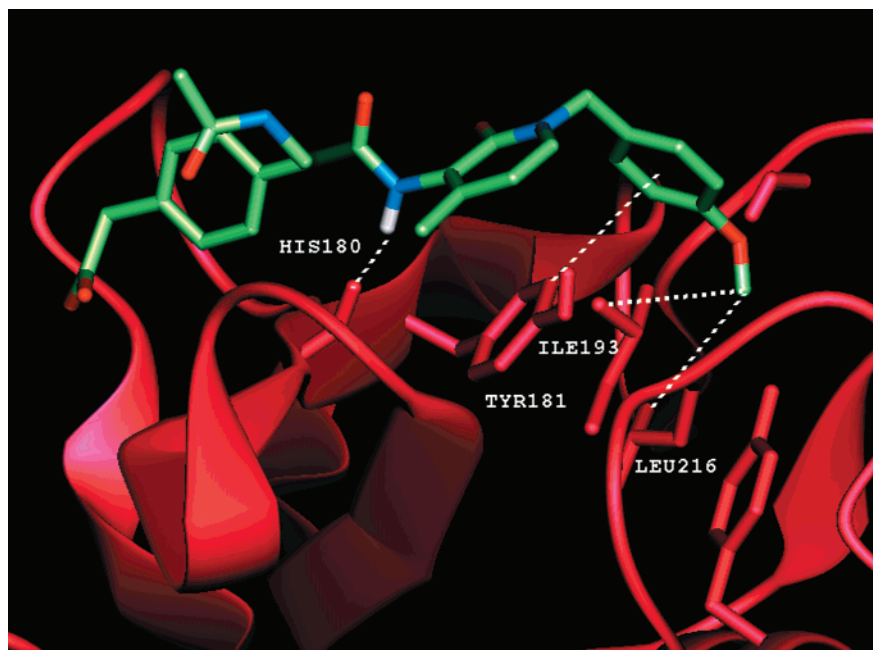


**Figure 2.** Some interactions of compound **6** with the p56lck SH2 domain.

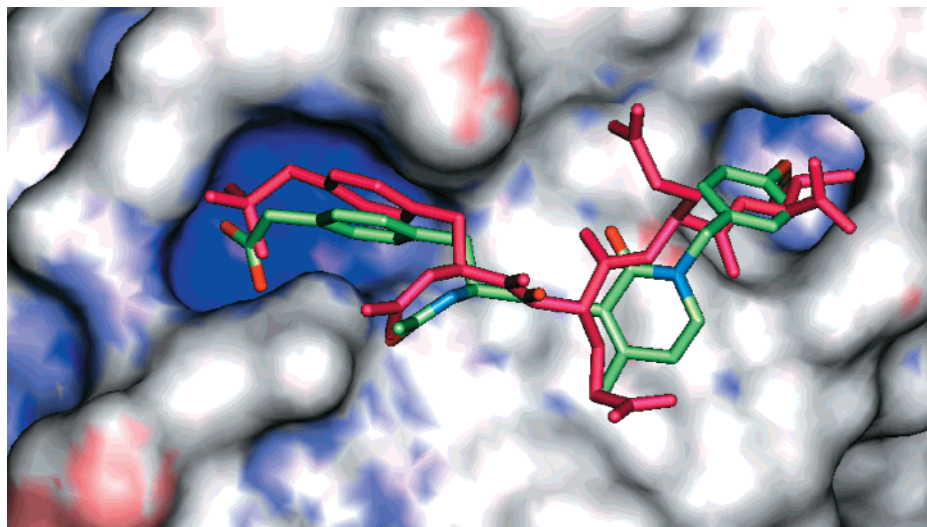


**Figure 3.** Overlap of compound **6** and AcpYEEI bound to the p56lck SH2 domain.

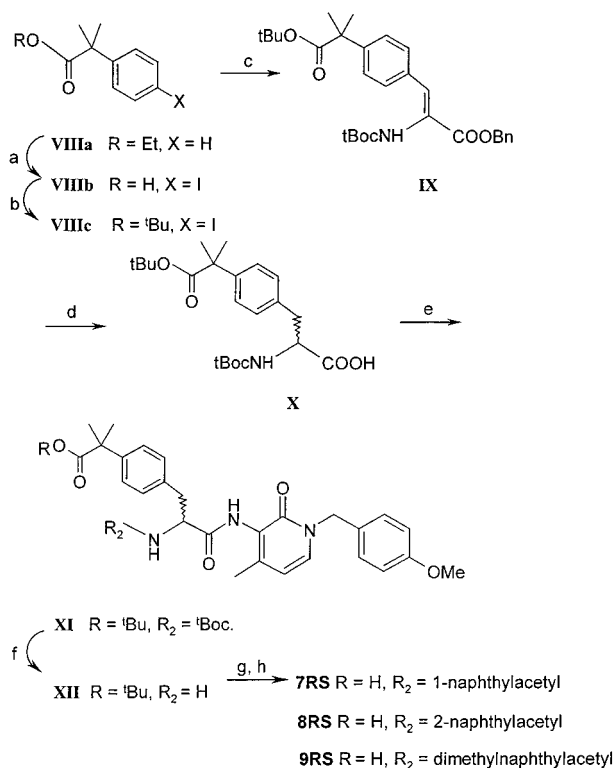
= 1.2  $\mu\text{M}$ ) with **5** ( $K_d = 1.3 \mu\text{M}$ ) shows that, while the additional methyl groups adjacent to the carboxyl group have little effect on binding affinity to the SH2 domain,<sup>29</sup> they improve cell permeation ( $22 \times 10^{-6}$  vs  $11 \times 10^{-6}$  cm/s when measured in the B→A direction, Table 1). The 2-naphthylacetyl analogue **8RS** shows a 3-fold enhancement in binding affinity ( $K_d = 0.3 \mu\text{M}$ ) with permeability properties equivalent to **7RS**. Note that both compounds are efflux pump substrates. Additional dimethyl substitution adjacent to the P-1 amide, illustrated with compound **9RS**, results in a small decrease in binding affinity versus **8RS** (**9RS**  $K_d = 1.2 \mu\text{M}$ , **8RS**  $K_d = 0.3 \mu\text{M}$ ) and improved cell permeation over **8RS** in the A→B direction ( $6 \times 10^{-6}$  vs  $0.19 \times 10^{-6}$  cm/s). This indication of further improved permeability along with good affinity prompted the resolution of **9RS** by chiral HPLC into enantiomers **9R** and **9S**. The S enantiomer, **9S**, was identified as the active enantiomer,<sup>30</sup> and permeation data in the B→A Caco-2 experi-

ment confirmed the expected good cell permeability properties.

### Inhibition of Ca Influx

Now that we had demonstrated good binding affinity along with acceptable cell permeability in compound **9S**, we wanted to show as conclusively as possible that our compounds would inhibit T cell activation by the intended mechanism, i.e., binding to the lck SH2 domain. It is not uncommon for compounds to cause unpredicted effects when tested in cell based assays, so we felt it would be prudent to test the much less active enantiomer **9R** as a control along with **9S**. This would increase our confidence that we were inhibiting by the desired mechanism.

Engagement of the T cell receptor (TCR) leads to an increase in cytosolic calcium levels resulting from the release of calcium from intracellular stores and subsequent influx of extracellular calcium. An antagonist of

Scheme 4<sup>a</sup>

<sup>a</sup> Conditions: (a) I<sub>2</sub>, NaIO<sub>3</sub>, concentrated H<sub>2</sub>SO<sub>4</sub>, AcOH, 55 °C; (b) oxalyl chloride, DMF, CH<sub>2</sub>Cl<sub>2</sub>, KO<sup>t</sup>Bu; (c) Pd(OAc)<sub>2</sub>, NaHCO<sub>3</sub>, (Bu)<sub>4</sub>NCl, DMF, benzyl (2-<sup>t</sup>butoxycarbonylamino)acrylate; (d) Pd/C, ethanol; (e) EDC, CH<sub>2</sub>Cl<sub>2</sub>, **IIb**; (f) HCl/dioxane; (g) EDC, appropriate carboxylic acid, CH<sub>2</sub>Cl<sub>2</sub>; (h) TFA.

Table 2

compd	inhibition of Ca <sup>2+</sup> influx in Jurkat T cells (EC <sub>50</sub> , μM)	inhibition of IL-2 production from CD4 <sup>+</sup> T cells (EC <sub>50</sub> , μM)	inhibition of proliferation of CD4 <sup>+</sup> T cells (EC <sub>50</sub> , μM)
<b>3</b>	> 100		
<b>5</b>	> 100		
<b>7RS</b>	51.0 ± 16.1 (n = 4)		
<b>8RS</b>	30.5 ± 2.9 (n = 4)		
<b>9S</b>	10.1 ± 0.8 (n = 4)	9.4 ± 4.2 (n = 9)	8.7 ± 3.6 (n = 4)
<b>9R</b>	29% inhibition @ 50 μM 57% inhibition @ 50 μM	11.3 ± 1.0 (n = 3)	16.6 ± 4.8 (n = 3)

the lck SH2 domain should abrogate the release of calcium from intracellular stores and prevent the influx of extracellular calcium. The ability of the two enantiomers **9S** and **9R** to inhibit the function of the lck SH2 domain in intact cells was assessed in Jurkat cells (a human T cell leukemic line), loaded with the calcium-sensitive indicator dye, Fluo-3. Changes in fluorescence following antibody mediated TCR cross-linking were monitored over time. Compound **9S** inhibited receptor-mediated increase in intracellular calcium concentration with an EC<sub>50</sub> of 10 μM (Table 2). Application of the inactive enantiomer **9R** had a substantially weaker effect on the activation induced calcium influx (EC<sub>50</sub> > 50 μM), supporting action of **9S** via antagonism of the lck SH2 domain. In addition, **9S** had no effect on calcium influx induced by a T cell receptor independent mechanism, that of treatment with the calcium ATPase inhibitor thapsigargin<sup>31</sup> (data not shown). Since the results from the calcium assay and from phosphorylation experiments (to be published in a separate account)<sup>32</sup> showed efficacy that was enantiomer and TCR

signaling dependent, there is strong evidence that compound **9S** inhibits the early events of T cell signal transduction via the intended mechanism.

Activation of the receptor mediated signal transduction pathway can lead to the induction of multiple genes and ultimately to cellular proliferation. The effects of compounds **9R** and **9S** on the synthesis and secretion of one of these gene products, IL-2, was also examined. Human CD4<sup>+</sup> T lymphocytes, purified from isolated peripheral blood mononuclear cells, were stimulated with antibodies to CD3 and CD28 in the presence or absence of compound. Following an overnight incubation, the cell supernatants were removed, and secreted IL-2 was quantified by ELISA. Compound **9S** inhibited IL-2 secretion in a dose dependent fashion with an IC<sub>50</sub> of 9.4 μM (Table 2). However, the enantiomer **9R**, which binds much less effectively to the lck SH2 domain, also blocked cytokine secretion to a similar extent. Comparable results were obtained for the two compounds when inhibition of cell proliferation was monitored. The similar profile for the two enantiomers in this longer duration assay suggests that nonspecific effects may be occurring in addition to the early effects on T cell activation.

## Conclusion

Recently, several research groups have tackled the problem of designing cell permeable ligands for various SH2 domains. Given the nature of the natural ligands, i.e., multiply charged phospho-peptides, this has proven to be a difficult task. We have shown that it is possible to design ligands for the p56lck SH2 domain that have binding affinity in the low micromolar range and that possess good cell permeability. Our success derives from a decision to pursue inhibitors that contain no more than one negative charge at physiological pH and from commitment to lessen the peptidic character of the lead molecules. The net result of our efforts is the transformation of a metabolically unstable, quintuply charged tetrapeptide **1** into an essentially nonpeptidic, monocharged species, **9S**. This molecule displays good binding affinity ( $K_d = 1 \mu\text{M}$ ) and good cell permeation properties. This combination of binding affinity and cell permeability allowed us to demonstrate clear-cut inhibitory effects on a very early event in T cell activation, namely calcium mobilization.

## Experimental Details

General experimental details have been previously described.<sup>7a,7b</sup>

**1-(4-Methoxybenzyl)-4-methyl-3-nitro-2-pyridone (IIb).** To a stirred suspension of **IIb** (2.0 g, 13 mmol) in DMF (60 mL) was added NaH (60% suspension in oil, 0.52 g). After 1 h, 4-methoxybenzyl chloride (1.8 mL) was added, and the mixture was stirred overnight at room temperature. Ethyl acetate was added, and the organic phase was washed with water, dried, filtered, and evaporated. Chromatography of the residue over silica gel (ethyl acetate/hexane) gave **IIb** (2.0 g, 7.3 mmol, 56%): <sup>1</sup>H NMR δ CDCl<sub>3</sub> 7.30–7.26 (3H), 6.89 (2H, d, *J* = 9), 6.05 (1H, d, *J* = 7), 5.08 (2H, s), 3.80 (3H, s), 2.24 (3H, s); MS(CI) 275 (MH<sup>+</sup>). Anal. (C<sub>14</sub>H<sub>14</sub>N<sub>2</sub>O<sub>4</sub>) C, H, N.

**3-Amino-1-(4-methoxybenzyl)-4-methyl-2-pyridone (IIb).** A mixture of **IIb** (1.5 g, 5.5 mmol) and 10% Pd/C (0.15 g) in ethanol (150 mL) was hydrogenated at 40 psi in a Parr apparatus for 5.5 h. The catalyst was removed by filtration,

and the solvent was evaporated to give **IIIb** (1.3 g, 5.3 mmol, 96%):  $^1\text{H NMR } \delta$   $\text{CDCl}_3$  7.24 (2H, d,  $J = 9$ ), 6.85 (2H, d,  $J = 9$ ), 6.69 (1H, d,  $J = 7$ ), 5.97 (1H, d,  $J = 7$ ), 5.08 (2H, s), 4.04 (2H, br s), 3.78 (3H, s), 2.04 (3H, s); MS(CI) 245 ( $\text{MH}^+$ ). Anal. ( $\text{C}_{14}\text{H}_{16}\text{N}_2\text{O}_2$ ) C, H, N.

**3-Amino-1-(4-methoxybenzyl)-2-pyridone (IIIa)** was synthesized in an analogous manner:  $^1\text{H NMR } \delta$   $\text{CDCl}_3$  7.26 (2H, d,  $J = 9$ ), 6.86 (2H, d,  $J = 9$ ), 6.72 (1H, dd,  $J = 2, 7$ ), 6.50 (1H, dd,  $J = 2, 7$ ), 6.04 (1H, apparent t,  $J = 7$ ), 5.10 (2H, s), 4.22 (2H, br s), 3.78 (3H, s); MS(CI) 231 ( $\text{MH}^+$ ). Anal. ( $\text{C}_{13}\text{H}_{14}\text{N}_2\text{O}_2$ ) C, H, N.

**2,2-Dimethyl-2-naphthylacetic Acid. 2-Naphthylacetic Acid Benzyl Ester.** To a stirred solution of 2-naphthylacetic acid (1 g, 5.4 mmol) in acetonitrile (10 mL) were added DBU (0.97 mL, 6.4 mmol) and benzyl bromide (0.77 mL, 6.4 mmol). After 3 h, the mixture was concentrated, and the residue was taken up in ethyl acetate. The organic phase was washed with 10% citric acid, 10%  $\text{NaHCO}_3$ , and brine, dried ( $\text{MgSO}_4$ ), and concentrated to give 2-naphthylacetic acid benzyl ester as a white solid (1.5 g, 100%).

**2,2-Dimethyl-(2-naphthyl)acetic Acid Benzyl Ester.** 2-Naphthylacetic acid benzyl ester (0.750 g, 2.72 mmol) in THF (4 mL) was slowly added to a cold (0 °C) solution of sodium bis(trimethylsilyl)amide (1 M in THF, 4.1 mL) and iodomethane (0.25 mL). After 30 min at room temperature, additional sodium bis(trimethylsilyl)amide (4.1 mL) and iodomethane (0.25 mL) were added. After 1 h, ethyl acetate was added, and the mixture was washed with 10% citric acid, 10%  $\text{NaHCO}_3$ , and brine. The solvent was evaporated, and flash column chromatography of the residue (10% ethyl acetate/hexane) gave 2,2-dimethyl-(2-naphthyl)acetic acid, benzyl ester as a colorless oil (0.46 g, 1.5 mmol, 55%).

**2,2-Dimethyl-(2-naphthyl)acetic Acid.** A mixture of 2,2-dimethyl-(2-naphthyl)acetic acid, benzyl ester (0.46 g, 1.5 mmol) and 10% Pd/C (0.040 g) in ethanol (5 mL) was hydrogenated at 1 atm for 16 h. The catalyst was removed by filtration, and the solvent was evaporated to give 2,2-dimethyl-(2-naphthyl)acetic acid (0.33 g, 1.5 mmol, 100%).

**3-[2'-(S)-(1'''-Naphthylacetyl)amino-3'-(4''-methoxycarbonylmethyl)benzene]propanoylamino-1-(4-methoxybenzyl)-4-methyl-2-pyridone (Vb).** A mixture of **IV**<sup>7b,23</sup> (1.0 g, 3 mmol) and EDC (0.63 g, 3.3 mmol) in methylene chloride (5 mL) was stirred at 0 °C for 20 min. 3-Amino-1-(4-methoxybenzyl)-4-methyl-2-pyridone (**IIIb**) (0.80 g, 3.3 mmol) was added, and after 1 h, the mixture was allowed to warm to room temperature and was stirred at room temperature overnight. The mixture was diluted with ethyl acetate, washed with water, dried, filtered, and evaporated. Chromatography of the residue over silica gel (ethyl acetate/hexane 1/4) gave **Vb** (0.45 g, 0.80 mmol, 27%) as a noncrystalline solid:  $^1\text{H NMR } \delta$   $\text{CDCl}_3$  7.95 (1H, br s), 7.26–7.21 (6H, m), 7.06 (1H, d,  $J = 7$ ), 6.86 (2H, d,  $J = 8$ ), 6.06 (1H, d,  $J = 7$ ), 5.10 (1H, br), 5.07 (1H, d,  $J = 15$ ), 5.00 (1H, d,  $J = 15$ ), 4.59 (1H, m), 3.79 (3H, s), 3.68 (3H, s), 3.58 (2H, s), 3.27 (1H, m), 3.08 (1H, m), 2.08 (3H, s), 1.38 (9H, s); MS(EI) 563 ( $\text{M}^+$ ). Anal. ( $\text{C}_{31}\text{H}_{37}\text{N}_3\text{O}_7$ ) C, H, N.

**3-[2'-(S)-(1'''-Naphthylacetyl)amino-3'-(4''-methoxycarbonylmethyl)benzene]propanoylamino-1-(4-methoxybenzyl)-2-pyridone (Va)** was obtained as a noncrystalline solid in an analogous manner using **IIIa** as a coupling partner:  $^1\text{H NMR } \delta$   $\text{CDCl}_3$  8.93 (1H, br s), 8.34 (1H, dd,  $J = 2, 7$ ), 7.22–7.12 (6H, m), 7.00 (1H, dd,  $J = 2, 7$ ), 6.86 (2H, d,  $J = 9$ ), 6.20 (1H, apparent t,  $J = 7$ ), 5.08–5.02 (3H, d), 4.54 (1H, br), 3.77 (3H, s), 3.67 (3H, s), 3.57 (2H, s), 3.20 (1H, dd,  $J = 6, 9$ ), 3.05 (1H, m), 1.38 (9H, s). Anal. ( $\text{C}_{30}\text{H}_{35}\text{N}_3\text{O}_7$ ) C, H, N.

**3-[2'-(S)-Amino-3'-(4''-methoxycarbonylmethyl)benzene]propanoylamino-1-(4-methoxybenzyl)-4-methyl-2-pyridone (VIb).** To a solution of **Vb** (0.40 g, 0.71 mmol) in methylene chloride (3 mL) was added TFA, and the mixture was stirred at room temperature overnight. The solvents were evaporated, and the residue was taken up in methylene chloride and aqueous sodium bicarbonate. The organic phase was dried ( $\text{Na}_2\text{SO}_4$ ), filtered, and evaporated. Chromatography of the residue over silica gel (methylene chloride/methanol) gave **VIb** (0.40 g, 0.86 mmol, >100%) as a sticky solid which

was taken on directly to the next step:  $^1\text{H NMR } \delta$   $\text{CDCl}_3$  9.33 (1H, br s), 7.28–7.25 (6H, m), 7.09 (1H, d,  $J = 7$ ), 6.88 (2H, d,  $J = 9$ ), 6.75 (2H, d,  $J = 8$ ), 6.10 (1H, d,  $J = 7$ ), 5.07 (2H, m), 3.81 (3H, s), 3.81 (1H, m), 3.72 (3H, s), 3.64 (2H, s), 3.35 (1H, m), 2.77 (1H, m), 2.16 (3H, s); MS(EI) 463 ( $\text{M}^+$ ). Anal. ( $\text{C}_{26}\text{H}_{29}\text{N}_3\text{O}_5$ ) C, H, N.

**3-[2'-(S)-(1'''-Naphthylacetyl)amino-3'-(4''-methoxycarbonylmethyl)benzene]propanoylamino-1-(4-methoxybenzyl)-4-methyl-2-pyridone (VIIb).** To a stirred solution of 1-naphthylacetic acid (0.041 g, 0.22 mmol) in methylene chloride (2 mL) cooled on ice was added EDC (0.046 g, 0.24 mmol). After 20 min, **VIb** (0.10 g, 0.22 mmol) in methylene chloride (1 mL) was added, followed by Hunig's base (0.03 g). The mixture was stirred on ice for 1 h and allowed to warm to room temperature overnight. The mixture was diluted with ethyl acetate, washed with water, dried, filtered, and evaporated. Chromatography of the residue over silica gel (methylene chloride/methanol, 19/1) gave **VIIb** (0.12 g, 0.19 mmol, 86%): mp 154–155 °C;  $^1\text{H NMR } \delta$   $\text{CDCl}_3$  7.93–7.78 (4H, m), 7.51–7.34 (4H, m), 7.24 (2H, d,  $J = 9$ ), 7.06 (1H, d,  $J = 7$ ), 6.93 (2H, d,  $J = 8$ ), 6.89 (2H, d,  $J = 9$ ), 6.75 (2H, d,  $J = 8$ ), 6.04 (1H, d,  $J = 7$ ), 5.96 (1H, d,  $J = 8$ ), 5.05 (2H, s), 4.85 (1H, m), 4.04 (2H, m), 3.82 (3H, m), 3.71 (3H, s), 3.53 (2H, s), 2.99–2.80 (2H, m), 2.00 (3H, s); MS(CI) 632 ( $\text{MH}^+$ ). Anal. ( $\text{C}_{38}\text{H}_{37}\text{N}_3\text{O}_6 \cdot 0.5\text{H}_2\text{O}$ ) C, H, N.

**3-[2'-(S)-(1'''-Naphthylacetyl)amino-3'-(4''-carboxymethyl)benzene]propanoylamino-1-(4-methoxybenzyl)-4-methyl-2-pyridone (5).** To a solution of **VIIb** (0.07 g, 0.11 mmol) in methanol/THF (1/1, 5 mL) was added aqueous NaOH (1 M, 0.15 mL). The mixture was stirred at room temperature overnight and acidified with 1 M aqueous HCl. The solvents were evaporated, and the residue was taken up in ethyl acetate/water. The organic phase was dried, filtered, and evaporated to give **5** (0.065 g, 0.11 mmol, 100%): mp 224–226 °C (ethyl acetate/methanol);  $^1\text{H NMR } \delta$  DMSO 9.48 (1H, s), 8.51 (1H, d,  $J = 8$ ), 7.88–7.13 (14H, m), 7.51–7.34 (4H, m), 6.89 (2H, d,  $J = 9$ ), 6.15 (1H, d,  $J = 7$ ), 5.03 (2H, m), 4.75 (1H, m), 3.89 (2H, m), 3.73 (3H, s), 3.53 (2H, s), 3.21 (1H, m), 2.87 (1H, m), 1.88 (3H, s). Anal. ( $\text{C}_{37}\text{H}_{35}\text{N}_3\text{O}_6 \cdot \text{H}_2\text{O}$ ) C, H, N.

**3-[2'-(S)-Acetylamino-3'-(4''-carboxymethyl)benzene]propanoylamino-1-(4-methoxybenzyl)-4-methyl-2-pyridone (6).** To a solution of **VIb** (0.10 g, 0.22 mmol) in methylene chloride (2 mL), cooled on ice, was added a few drops of Hunig's base followed by acetic anhydride (0.045 g). The mixture was allowed to warm to room temperature overnight. The solvent was evaporated, and the residue was triturated with ether and collected by filtration to give **VIc**: mp 158–159 °C;  $^1\text{H NMR } \delta$   $\text{CDCl}_3$  7.82 (1H, s), 7.28–7.22 (6H, m), 7.08 (1H, d,  $J = 7$ ), 6.89 (2H, d,  $J = 8$ ), 6.22 (1H, d,  $J = 8$ ), 6.09 (1H, d,  $J = 7$ ), 5.08 (1H, d,  $J = 14$ ), 5.03 (1H, d,  $J = 4$ ), 4.95 (1H, m), 3.81 (3H, m), 3.70 (3H, s), 3.61 (2H, s), 3.25–3.18 (2H, m), 2.07 (3H, s), 2.02 (3H, s); MS(CI) 506 ( $\text{MH}^+$ ). Anal. ( $\text{C}_{28}\text{H}_{31}\text{N}_3\text{O}_6 \cdot 0.5\text{H}_2\text{O}$ ) C, H, N.

To a solution of **VIc** (0.065 g, 0.13 mmol), prepared above, in methanol (3 mL) was added aqueous NaOH (1 M, 0.14 mL). The mixture was stirred at room temperature overnight and acidified with 1 M aqueous HCl. The solvent was evaporated, and the residue was partitioned between ethyl acetate and water. The organic phase was separated, dried, filtered, and evaporated to give **6** (0.06 g, 0.012 mmol, 55% over two steps from **VIb**): mp 190–192 °C (ethyl acetate/methanol);  $^1\text{H NMR } \delta$  DMSO 9.40 (1H, s), 8.14 (1H, d,  $J = 8$ ), 7.63 (1H, d,  $J = 7$ ), 7.27 (4H, m), 7.15 (2H, d,  $J = 8$ ), 6.89 (2H, d,  $J = 9$ ), 6.14 (1H, d,  $J = 7$ ), 5.12 (2H, m), 4.74 (1H, m), 3.72 (3H, s), 3.51 (2H, s), 3.08 (1H, m), 2.78 (1H, m), 1.88 (3H, s), 1.76 (3H, s); MS(EI) 491 ( $\text{M}^+$ ). Anal. ( $\text{C}_{27}\text{H}_{29}\text{N}_3\text{O}_6 \cdot 0.25\text{H}_2\text{O}$ ) C, H, N.

**3-[2'-(S)-Amino-3'-(4''-methoxycarbonylmethyl)benzene]propanoylamino-1-(4-methoxybenzyl)-2-pyridone Hydrochloride (VIa-HCl).** A solution of **Va** (0.62 g, 1.1 mmol) in 4 N HCl/dioxane (7.5 mL) was left at room temperature for 16 h. The solvent was evaporated. Ethyl acetate was added, and the solvent was evaporated to give the hydrochloride salt of **VIa** as a solid (0.52 g, 1.1 mmol):  $^1\text{H NMR } \delta$  DMSO 10.13 (1H, s), 8.37 (3H, br s), 8.18 (1H, dd,  $J = 2, 7$ ), 7.64 (1H, dd,  $J$

= 2, 7), 7.32 (2H, d,  $J = 9$ ), 7.27–7.19 (4H, m), 6.91 (2H, d,  $J = 9$ ), 6.32 (1H, apparent t,  $J = 7$ ), 5.10 (m, 2H), 4.57 (m, 1H), 3.73 (3H, s), 3.64 (2H, s), 3.60 (3H, s), 3.18–3.02 (2H, m); MS-(CI) 450. Anal. ( $C_{25}H_{27}N_3O_5 \cdot HCl \cdot H_2O$ ) C, H, N.

**3-[2'-(S)-(1'''-Naphthylacetyl)amino-3'-(4''-methoxycarbonylmethyl)benzene]propanoylamino-1-(4-methoxybenzyl)-2-pyridone (VIIa).** To a solution of 1-naphthylacetic acid (0.21 g, 0.11 mmol) in methylene chloride (2 mL) cooled on ice was added EDC (0.22 g, 0.11 mmol). After 15 min, **VIa-HCl** (0.40 g, 0.82 mmol) in methylene chloride (10 mL) was added. After 3 h at room temperature, the mixture was fractionated directly over silica gel (methylene chloride to methylene chloride/ethyl acetate 3/1) to give **VIIa** (0.31 g, 0.50 mmol, 61%): mp 151–153 °C (ethyl acetate/hexane);  $^1H$  NMR  $\delta$   $CDCl_3$  8.85 (1H, s), 8.25 (1H, dd,  $J = 2, 7$ ), 7.92–7.23 (9H, m), 6.99 (1H, dd,  $J = 2, 7$ ), 6.90 (2H, d,  $J = 9$ ), 6.85 (2H, d,  $J = 9$ ), 6.54 (2H, d,  $J = 8$ ), 6.22 (1H, d,  $J = 8$ ), 6.18 (1H, apparent t,  $J = 7$ ), 5.80 (1H, d,  $J = 8$ ), 5.11 (2H, s), 4.79 (1H, m), 4.09 (1H, d,  $J = 16$ ), 4.00 (1H, d,  $J = 16$ ), 3.80 (3H, m), 3.69 (3H, s), 3.49 (2H, s), 2.88 (2H, d,  $J = 6$ ); Anal. ( $C_{38}H_{37}N_3O_6$ ) C, H, N.

**3-[2'-(S)-(1'''-Naphthylacetyl)amino-3'-(4''-carboxymethyl)benzene]propanoylamino-1-(4-methoxybenzyl)-2-pyridone (4).** To a stirred solution of **VIIa** (0.15 g, 0.24 mmol) in THF (3 mL) was added a solution of lithium hydroxide hydrate (0.013 g) in water (0.3 mL). After 3.5 h at room temperature, ethyl acetate and aqueous sodium bicarbonate were added. The aqueous phase was separated, acidified with 1 N  $KHSO_4$ , and extracted with ethyl acetate. The organic phase was dried, filtered, and evaporated. Trituration with ether gave **4** (0.076 g, 0.12 mmol, 50%) as a solid that was collected by filtration: mp 187–190 °C;  $^1H$  NMR  $\delta$  DMSO 9.53 (1H, s), 8.75 (1H, d,  $J = 8$ ), 8.23 (1H, dd,  $J = 2, 7$ ), 7.89–7.85 (2H, m), 7.77 (1H, d,  $J = 8$ ), 7.57 (1H, dd,  $J = 2, 7$ ), 7.45 (1H, t,  $J = 7$ ), 7.38–7.13 (9H, m), 6.91 (2H, d,  $J = 9$ ), 6.31 (1H, apparent t,  $J = 7$ ), 5.12 (2H, s), 4.77 (1H, m), 3.91 (2H, s), 3.74 (3H, s), 3.34 (2H, s), 3.12 (1H, m), 2.88 (1H, m). Anal. ( $C_{36}H_{33}N_3O_6 \cdot 0.5H_2O$ ) C, H, N.

**4-Iodo-(1'-butoxycarbonyl-1'-methyl)ethylbenzene (VI-Ic).** To a stirred solution of ethyl phenylacetate (32.8 g, 200 mmol) in THF (1 L) under argon was added sodium bistrimethylsilylamide (2 M in THF, 100 mL). After 45 min, methyl iodide (13 mL) was added over 15 min. After 30 min, additional sodium bistrimethylsilylamide (2 M in THF, 100 mL) was added, followed, after 30 min, by methyl iodide (14 mL). After 30 min, the mixture was diluted with hexane and washed with water. The organic phase was dried, filtered, and evaporated to give (1'-ethoxycarbonyl-1'-methyl)ethylbenzene (**VIIIa**) (28.0 g, 146 mmol, 73%) which was taken on directly to the next step. A mixture of **VIIIa** (28.0 g, 146 mmol), iodine (24.7 g), sodium iodate (7.1 g), and concentrated sulfuric acid (4 mL) in acetic acid (200 mL) was stirred and heated at 55 °C for 90 h. The solvent was evaporated, and the residue was partitioned between water and hexane. The organic phase was washed with aqueous sodium thiosulfate, dried, filtered, and evaporated. The residue was taken up in ethanol (200 mL) and water (100 mL), and potassium hydroxide (20 g) was added. The mixture was heated under reflux for 5 h and cooled to room temperature. The mixture was washed with hexane. The aqueous phase was acidified with concentrated hydrochloric acid and extracted with hexane. The organic phase was dried, filtered, and evaporated to give 4-iodo-(1'-carboxy-1'-methyl)ethylbenzene (**VIIIb**) as a solid (19.6 g, 67 mmol, 46%): mp 106–110 °C (hexane);  $^1H$  NMR  $\delta$   $CDCl_3$  7.66 (2H, d,  $J = 8$ ), 7.15 (2H, d,  $J = 8$ ), 1.57 (6H, s). Anal. ( $C_{10}H_{11}O_2I$ ) C, H.

To a solution of **VIIIb** (18.7 g, 64.3 mmol) in methylene chloride (150 mL) was added dimethylformamide (0.5 mL) followed by oxalyl chloride (10 mL), dropwise. After 1 h, the solvent was evaporated, and the residue was taken up in THF (100 mL) and cooled on ice. Potassium <sup>t</sup>butoxide (1 M in THF, 75 mL) was added over 20 min. The mixture was diluted with hexane, washed with water, dried, filtered, and evaporated. The residue was triturated with methanol/water to give 4-iodo-(1'-<sup>t</sup>butoxycarbonyl-1'-methyl)ethylbenzene (**VIIIc**) as a solid

(18.1 g, 52.1 mmol, 81%): mp 60–62 °C;  $^1H$  NMR  $\delta$   $CDCl_3$  7.63 (2H, d,  $J = 8$ ), 7.09 (2H, d,  $J = 8$ ), 1.58 (6H, s), 1.37 (9H, s). Anal. ( $C_{14}H_{19}O_2I$ ) C, H.

**2'-Butoxycarbonylamino-3-[4'-(1'''-<sup>t</sup>butoxycarbonyl-1''-methyl)ethyl]benzenepropanoic Acid, Benzyl Ester (IX).** A mixture of benzyl (2'-butoxycarbonylamino)acrylate (8.00 g, 27.9 mmol), **VIIIc** (7.03 g, 20.3 mmol), sodium bicarbonate (4.03 g), tetrabutylammonium chloride hydrate (6.47 g), and palladium acetate (0.41 g) in dimethylformamide (10 mL) was degassed and covered with argon three times. The mixture was heated under argon at 80 °C for 5 h, cooled, diluted with ethyl acetate/hexane, and washed with water. The organic phase was dried, filtered, and evaporated. Chromatography of the residue over silica gel (ethyl acetate/hexane 98/2 to 9/1) gave **IX** as an oil that solidified upon trituration with hexane (7.24 g, 14.6 mmol, 72%): mp 81–83 °C;  $^1H$  NMR  $\delta$   $CDCl_3$  7.51–7.28 (9H, m), 6.13 (1H, br), 5.28 (1H, s), 1.51 (6H, s), 1.36 (9H, s); MS(EI) 495 ( $M^+$ ). Anal. ( $C_{29}H_{37}NO_6$ ) C, H, N.

**2-(R,S)-Butoxycarbonylamino-3-[4'-(1'''-<sup>t</sup>butoxycarbonyl-1''-methyl)ethyl]benzenepropanoic Acid (X).** A mixture of **IX** (7.39 g, 14.9 mmol) and 10% Pd/C (0.20 g) in ethanol (75 mL) was hydrogenated at 45 psi in a Parr apparatus for 26 h. The catalyst was removed by filtration, and the solvent was evaporated. The residue crystallized from hexane giving **X** (4.67 g, 11.5 mmol, 77%): mp 105–107 °C;  $^1H$  NMR  $\delta$   $CDCl_3$  7.28 (2H, d,  $J = 8$ ), 7.13 (2H, d,  $J = 8$ ), 4.92 (1H, d,  $J = 8$ ), 4.59 (1H, m), 3.19–3.05 (2H, m), 1.51 (6H, s), 1.41 (9H, s), 1.37 (9H, s); MS(CI) 425 ( $M + NH_4^+$ ). Anal. ( $C_{22}H_{33}NO_6$ ) C, H, N.

**3-[2'-(R,S)-<sup>t</sup>Butoxycarbonylamino-3'-[4'-(1'''-<sup>t</sup>butoxycarbonyl-1''-methyl)ethyl]benzene]propanoylamino-1-(4-methoxybenzyl)-4-methyl-2-pyridone (XI).** To a stirred solution of **X** (1.56 g, 3.83 mmol) in methylene chloride (5 mL) at 0 °C was added EDC (0.80 g, 4.2 mmol). After 10 min **IIIb** (1.16 g, 4.75 mmol) was added, and the mixture was stirred at room temperature for 4 h. Additional EDC (0.21 g) was added, and the mixture was stirred for 2 days. The mixture was fractionated directly over silica gel ( $CH_2Cl_2$  to 10% EtOAc/ $CH_2Cl_2$ ) to give **XI** (1.63 g, 2.57 mmol, 67%): mp 134–136 °C ( $Et_2O$ );  $^1H$  NMR  $\delta$   $CDCl_3$  7.96 (1H, br s), 7.28–7.16 (6H, m), 7.06 (1H, d,  $J = 7$ ), 6.86 (2H, d,  $J = 9$ ), 6.06 (1H, d,  $J = 7$ ), 5.08 (1H, br), 5.07 (1H, d,  $J = 14$ ), 5.00 (1H, d,  $J = 14$ ), 4.59 (1H, m), 3.79 (3H, s), 3.28 (1H, m), 3.05 (1H, m), 2.07 (3H, s), 1.49 (6H, s), 1.38 (9H, s), 1.35 (9H, s). Anal. ( $C_{36}H_{47}N_3O_7$ ) C, H, N.

**3-[2'-(R,S)-Naphthylacetylamino-3'-[4'-(1'''-carboxy-1''-methyl)ethyl]benzene]propanoylamino-1-(4-methoxybenzyl)-4-methyl-2-pyridone (8RS).** To a solution of **XI** (0.32 g) in dioxane (0.5 mL) cooled on ice was added HCl in dioxane (4 M, 1 mL). The mixture was allowed to warm to room temperature over 45 min, then diluted with ethyl acetate, washed with aqueous sodium bicarbonate, dried ( $Na_2SO_4$ ), filtered, and evaporated. The **XII** (0.30 g) obtained was carried on directly to the next step. To a stirred solution of **XII** (0.30 g) in  $CH_2Cl_2$  (3 mL) at room temperature were added 2-naphthylacetic acid (0.095 g) and EDC (0.098 g). After 1 h, the mixture was diluted with ethyl acetate, washed with water, dried, filtered, and evaporated, and the residue was taken up in TFA. After 2 h, the TFA was removed by evaporation, and the residue, dissolved in ethyl acetate, was washed with water, dried, filtered, and evaporated. Chromatography of the residue over silica gel ( $CH_2Cl_2$ /EtOH/AcOH 97/2.5/0.5) gave **8RS** (0.14 g) as an oil that solidified on trituration with ether: mp 208–210 °C ( $Et_2O$ / $CH_2Cl_2$ );  $^1H$  NMR  $\delta$   $CDCl_3$  8.81 (1H, br s), 7.12–7.73 (12H, m), 6.89 (4H, m), 6.27 (1H, d,  $J = 7$ ), 6.14 (1H, d,  $J = 7$ ), 5.07 (2H, s), 4.82 (1H, m), 3.80 (3H, s), 3.45 (2H, s), 3.11 (1H, m), 2.78 (1H, m), 2.00 (3H, s), 1.58 (3H, s), 1.56 (3H, s). Anal. ( $C_{39}H_{39}N_3O_6$ ) C, H, N.

**7RS** was prepared in an analogous manner: mp 149–151 °C ( $Et_2O$ / $CH_2Cl_2$ );  $^1H$  NMR  $\delta$   $CDCl_3$  8.80 (1H, br s), 7.08–7.81 (12H, m), 6.87 (2H, d,  $J = 9$ ), 6.72 (2H, d,  $J = 8$ ), 6.14 (2H, m), 5.07 (2H, s), 4.79 (1H, m), 3.80 (3H, s), 3.80 (1H, d,  $J = 16$ ), 3.71 (1H, d,  $J = 16$ ), 3.01 (1H, m), 2.68 (1H, m), 1.97 (3H, s), 1.59 (3H, s), 1.57 (3H, s). Anal. ( $C_{39}H_{39}N_3O_6 \cdot 0.25H_2O$ ) C, H, N.



**3-[2'-(*R,S*)-(Dimethyl)-naphthylacetyl-amino-3'-[4''-(1'''-carboxy-1'''-methyl)ethyl]benzene]propanoylamino-1-(4-methoxybenzyl)-4-methyl-2-pyridone (9RS)**: was prepared in an analogous manner using 2,2-dimethylnaphthylacetic acid in the coupling reaction: mp 157–161 °C (Et<sub>2</sub>O/CH<sub>2</sub>Cl<sub>2</sub>); <sup>1</sup>H NMR δ CDCl<sub>3</sub> 8.66 (1H, br s), 7.01–7.79 (12H, m), 6.87 (2H, d, *J* = 8), 6.69 (2H, d, *J* = 8), 6.14 (1H, d, *J* = 7), 5.95 (1H, d, *J* = 7), 5.07 (1H, d, *J* = 14), 5.00 (1H, d, *J* = 14), 4.82 (1H, m), 3.79 (3H, s), 3.04 (1H, m), 2.67 (1H, m), 2.05 (3H, s), 1.56 (3H, s), 1.53 (6H, s), 1.41 (3H, s). Anal. (C<sub>41</sub>H<sub>43</sub>N<sub>3</sub>O<sub>6</sub>·0.5H<sub>2</sub>O), C, H, N.

**3-[2'-(*S*)-(Dimethyl)-naphthylacetyl-amino-3'-[4''-(1'''-carboxy-1'''-methyl)ethyl]benzene]propanoylamino-1-(4-methoxybenzyl)-4-methyl-2-pyridone (9S)**: mp 115–117 °C; MS 674 (MH<sup>+</sup>). Anal. (C<sub>41</sub>H<sub>43</sub>N<sub>3</sub>O<sub>6</sub>·2H<sub>2</sub>O) C, H, N. ee 99.6% by chiral HPLC.

**3-[2'-(*R*)-(Dimethyl)-naphthylacetyl-amino-3'-[4''-(1'''-carboxy-1'''-methyl)ethyl]benzene]propanoylamino-1-(4-methoxybenzyl)-4-methyl-2-pyridone (9R)**: mp 117–119 °C; MS 674 (MH<sup>+</sup>). Anal. (C<sub>41</sub>H<sub>43</sub>N<sub>3</sub>O<sub>6</sub>·2H<sub>2</sub>O) C, H, N. ee 98.7% by chiral HPLC.

**Caco-2 Permeability Assay.** Caco-2 cells, originating from a human colorectal carcinoma, were obtained from American Tissue Culture Collection, Rockville, MD. The cells were grown at 37 °C in an atmosphere of 5% CO<sub>2</sub> in Dulbecco's Modified Eagle Medium (DMEM) containing 10% fetal calf serum, 1% nonessential amino acids, penicillin (100 Units/ml), and streptomycin (100 μg/ml). All culture media and reagents were from Gibco BRL Products, Gaithersburg, MD.

Caco-2 cells were seeded at a density of 80 000 cells/cm<sup>2</sup> in six-well plates on polycarbonate filters (Costar, Transwell cell culture inserts, diameter 24.5 mm, pore size 3.0 μm) coated with rat tail collagen type I. The cells were allowed to grow and differentiate for up to 25 days. Cells of passage numbers 23 to 50 were used throughout.

Prior to permeability experiments, the culture medium was replaced with the transport medium, Hank's Balanced Salt Solution (HBSS), pH 7.4, and equilibrated for 30 min at 37 °C. All wells in six-well clusters received 2.5 mL of HBSS. Drug solutions were prepared in HBSS at a final concentration of 0.01 to 0.1 mM. All permeability experiments were performed in an incubator at 37 °C and an atmosphere of 5% CO<sub>2</sub>. To initiate permeability experiments, the apical side of the monolayers received 1.5 mL of drug solutions. The amount of solute permeated was determined by either moving the inserts to new wells containing fresh medium or taking a sample from the basolateral side and replacing it with fresh medium at discrete time intervals. Transport rates were then determined by plotting the cumulative amount permeated as a function of time. Samples were analyzed by HPLC (Hewlett-Packard, HP 1090). The apparent permeability coefficient,  $P_{\text{Caco-2}}$ , was then determined according to eq 1

$$P_{\text{Caco-2}} = J/AC_0 \quad (1)$$

where *J* was the rate of appearance of the drug in the receiver chamber, *C*<sub>0</sub> was the initial concentration of the solute in the donor chamber, and *A* was the surface area of the filter. Mass balance was calculated for each experiment. In all experiments, the mass balance was more than 90%. Mannitol permeability was used to assess the integrity of Caco-2 cell monolayers. Permeability coefficients were determined at least in triplicates, and the mean and standard deviations are reported.

**Calcium Influx Assay.** Jurkat T cells were suspended in RPMI 1640 with 1% bovine calf serum and 10 mM HEPES, pH 7.5, and loaded with 2 μM Fluo-3 AM (Molecular Probes, Inc.) in the presence of Pluronic F127 for 1 h at room temperature. The cells were washed and resuspended in Hank's Balanced Salt Solution supplemented with 10 mM HEPES, pH 7.5. Cells (4 × 10<sup>6</sup>) were placed in a cuvette and equilibrated to 37 °C. Compound was added, and the Jurkat cells were activated 80 s later by the addition of 2 μg of mouse anti-human CD3 antibody (Clone ×35, Immunotech) which

cross-linked the T cell receptor. Changes in cytoplasmic calcium concentration were monitored by measurement of fluorescence over time on a luminescence spectrometer (SLM Amico Bowman Series 2). The EC<sub>50</sub> values were calculated based on the percent of control fluorescence at six doses of compound.

**Activation of Human CD4+ T Cells.** Purified human CD4+ T lymphocytes were suspended in RPMI 1640 supplemented with 1% fetal bovine serum, nonessential amino acids, 1 mM sodium pyruvate, 0.29 mg/mL L-glutamine, penicillin, and streptomycin, and 5 × 10<sup>4</sup> cells were added per well to a 96-well flat bottom plate. Compounds were diluted from DMSO stock solutions into medium and added to the cells, and the mixtures were preincubated for 1 h at 37 °C. The cells were activated by the addition of 0.12 ng/well mouse anti-human CD3, 100 ng/well rat anti-human CD28 (Clone YTH913.12), and 2 × 10<sup>5</sup> goat anti-mouse IgG coated magnetic beads/well (Dyna) in a final volume of 210 μL/well. The cells were incubated at 37 °C in a humidified atmosphere of 5% CO<sub>2</sub> overnight. A total of 10 μL/well of conditioned medium was removed, and the amount of interleukin-2 secreted by the T cells was quantitated utilizing an ELISA kit (R&D Systems) according to the manufacturers instructions. To measure proliferation, the cells were pulse labeled 48 h following activation with 0.5 μCi/well [<sup>3</sup>H]-thymidine (Amersham) and incubated a further 18 h at 37 °C. The cells were harvested on a 96-well plate harvester, and the incorporated radiolabeled thymidine determined using a β-plate counter.

EC<sub>50</sub> values for either IL-2 production or proliferation were calculated from data fit to a sigmoidal curve using nonlinear regression techniques.

**Molecular Modeling.** The crystal structure of the p56lck SH2 domain complexed with Ac-(*p*-carboxymethyl)Phe-Glu-Glu-Ile<sup>17</sup> was used to provide the starting geometry. The initial position of the Ac-phenylacetic portion of the ligand was the same as in the crystal structure of the complex with the tetrapeptide. The pyridone and *p*-methoxybenzyl groups were modeled with manual docking procedures. As previously,<sup>7a,7b</sup> the *p*-methoxybenzyl group was oriented toward the P+3 pocket. This initial model was optimized by performing a molecular dynamics (MD) simulation (1 nanosecond (ns)) using CharmM.<sup>33</sup> The electrostatic Coulombic potential was computed with a distance dependent dielectric using CharmM charges for the protein, and MNDO ESP charges using MOPAC<sup>34</sup> for the ligand. The MD was carried out in explicit solvent, using a TIP3P<sup>35</sup> solvent cap of 25 Å around the inhibitor. In this MD protocol, all the atoms within 13 Å of the inhibitor were allowed to move freely. The rest of the protein was constrained using a potential harmonic constraint of 5 kcal/Å<sup>2</sup>, and the remaining solvent molecules were maintained within the sphere limit by applying the CharmM DROP restraint option. Several structures, as well as the average structure, were collected along the 1 ns trajectory for further analysis.

**Acknowledgment.** We thank Dr. Denice Spero, Dr. Xiao-Jun Wang, and Michel Emmanuel for assistance in the scale-up of various compounds. We also thank Kelli Chessic and Katherine Briggs for assistance in running the Caco-2 model.

## References

- Pawson, T. Protein modules and signaling networks. *Nature* **1995**, *373*, 573–580.
- (a) Gilmer, T.; Rodriguez, M.; Jordan, S.; Crosby, R.; Alligood, K.; Green, M.; Kimery, M.; Wagner, C.; Kinder, D.; Charifson, P.; Hassell, A. M.; Willard, D.; Luther, M.; Rusnak, D.; Sternbach, D. D.; Mehrotra, M.; Peel, M.; Shampine, L.; Davis, R.; Robbins, J.; Patel, I. R.; Kassel, D.; Burkhardt, W.; Moyer, M.; Bradshaw, T.; Berman, J. Peptide inhibitors of src SH3-SH2-phosphoprotein interactions. *J. Biol. Chem.* **1994**, *269*, 31711–31719. (b) Pacofsky, G. J.; Lackey, K.; Alligood, K. J.; Berman, J.; Charifson, P. S.; Crosby, R. M.; Dorsey, G. F., Jr.; Feldman, P. L.; Gilmer, T. M.; Hummel, C. W.; Jordan, S. R.; Mohr, C.; Shewchuk, L. M.; Sternbach, D. D.; Rodriguez, M. Potent dipeptide inhibitors of the pp60c-src SH2 domain. *J. Med. Chem.*

- 1998, 41, 1894–1908. (c) Charifson, P.; Shewchuk, L. M.; Rocque, W.; Hummel, C. W.; Jordan, S. R.; Mohr, C.; Pacofsky, G. J.; Peel, M. R.; Rodriguez, M.; Sternbach, D. D.; Consler, T. G. Peptide ligands of pp60c-src SH2 domains: A thermodynamic and structural study. *Biochemistry* **1997**, *36*, 6283–6293.
- (3) (a) Lunney, E. A.; Para, K. S.; Rubin, J. R.; Humblet, C.; Fergus, J. H.; Marks, J. S.; Sawyer, T. K. Structure-based design of a novel series of nonpeptide ligands that bind to the pp60src SH2 domain. *J. Am. Chem. Soc.* **1997**, *119*, 12471–12476. (b) Plummer, M. S.; Lunney, E. A.; Para, K. S.; Shahripour, A.; Stankovic, C. J.; Humblet, C.; Fergus, J. H.; Marks, J. S.; Herrera, R.; Hubbell, S.; Saltiel, A.; Sawyer, T. K. Design of peptidomimetic ligands for the pp60src SH2 domain. *Bioorg. Med. Chem.* **1997**, *5*, 41–47. (c) Stankovic, C. J.; Surendran, N.; Lunney, E. A.; Plummer, M. S.; Para, K. S.; Shahripour, A.; Fergus, J. H.; Marks, J. S.; Herrera, R.; Hubbell, S. E.; Humblet, C.; Saltiel, A. R.; Stewart, B. H.; Sawyer, T. K. The role of 4-phosphonodifluoromethyl- and 4-phosphono-phenylalanine in the selectivity and cellular uptake of SH2 domain ligands. *Bioorg. Med. Chem. Lett.* **1997**, *7*, 1909–1914. (d) Plummer, M. S.; Holland, D. R.; Shahripour, A.; Lunney, E. A.; Fergus, J. H.; Marks, J. S.; McConnell, P.; Mueller, W. T.; Sawyer, T. K. Design, synthesis, and cocrystal structure of a nonpeptide Src SH2 domain ligand. *J. Med. Chem.* **1997**, *40*, 3719–3725. (e) Shahripour, A.; Plummer, M. S.; Lunney, E. A.; Para, K. S.; Stankovic, C. J.; Rubin, J. R.; Humblet, C.; Fergus, J. H.; Marks, J. S.; Herrera, R.; Hubbell, S. E.; Saltiel, A. R.; Sawyer, T. K. Novel phosphotyrosine mimetics in the design of peptide ligands for pp60src SH2 domain. *Bioorg. Med. Chem. Lett.* **1996**, *6*, 1209–1214. (e) Shahripour, A.; Para, K. S.; Plummer, M. S.; Lunney, E. A.; Holland, D. R.; Rubin, J. R.; Humblet, C.; Fergus, J. H.; Marks, J. S.; Saltiel, A. R.; Sawyer, T. K. Structure-based design of novel dipeptide ligands targeting the pp60src SH2 domain. *Bioorg. Med. Chem. Lett.* **1997**, *7*, 1107–1112.
- (4) (a) Buchanan, J. L.; Bohacek, R. S.; Luke, G. P.; Hatada, M.; Lu, X.; Dalgarno, D. C.; Narula, S. S.; Yuan, R.; Holt, D. A. Structure-based design and synthesis of a novel class of src SH2 inhibitors. *Bioorg. Med. Chem. Lett.* **1999**, *9*, 2353–2358. (b) Buchanan, J. L.; Vu, C. B.; Merry, T. J.; Corpuz, E. G.; Pradeepan, S. G.; Mani, U. N.; Yang, M.; Plake, H. R.; Varkhedkar, V. M.; Lynch, B. A.; MacNeil, I. A.; Loiacono, K. A.; Tiong, C. L.; Holt, D. A. Structure–activity relationships of a novel class of src SH2 inhibitors. *Bioorg. Med. Chem. Lett.* **1999**, *9*, 2359–2364.
- (5) (a) Furet, P.; Garcia-Echeverria, C.; Gay, B.; Schoepfer, J.; Zeller, M.; Rahuel, J. Structure-based design, synthesis, and X-ray crystallography of a high-affinity antagonist of the Grb2-SH2 domain containing an asparagine mimetic. *J. Med. Chem.* **1999**, *42*, 2358–2363. (b) Furet, P.; Gay, B.; Caravatti, G.; Garcia-Echeverria, C.; Rahuel, J.; Schoepfer, J.; Fretz, H. Structure-based design and synthesis of high affinity tripeptide ligands of the Grb2-SH2 domain. *J. Med. Chem.* **1998**, *41*, 3442–3449. (c) Garcia-Echeverria, C.; Furet, P.; Gay, B.; Fretz, H.; Rahuel, J.; Schoepfer, J.; Caravatti, G. Potent antagonists of the SH2 domain of Grb2: optimization of the X+1 position of 3-amino-Z-tyr(PO3H2)-X+1-asn-NH2. *J. Med. Chem.* **1998**, *41*, 1741–1744. (d) Rahuel, J.; Garcia-Echeverria, C.; Furet, P.; Strauss, A.; Caravatti, G.; Fretz, H.; Schoepfer, J.; Gay, B. Structural basis for the high affinity of amino-aromatic SH2 phosphopeptide ligands. *J. Mol. Biol.* **1998**, *279*, 1013–1022. (e) Furet, P.; Gay, B.; Garcia-Echeverria, C.; Rahuel, J.; Fretz, H.; Schoepfer, J.; Caravatti, G. Discovery of 3-aminobenzoyloxycarbonyl as an N-terminal group conferring high affinity to the minimal phosphopeptide sequence recognized by the Grb2-SH2 domain. *J. Med. Chem.* **1997**, *40*, 3551–3556.
- (6) Yao, Z.-J.; King, C. R.; Cao, T.; Kelley, J.; Milne, G. W. A.; Voigt, J. H.; Burke, T. R., Jr. Potent inhibition of Grb2 SH2 domain binding by nonphosphate-containing ligands. *J. Med. Chem.* **1999**, *42*, 25–35.
- (7) (a) Llinas-Brunet, M.; Beaulieu, P. L.; Cameron, D. R.; Ferland, J.-M.; Gauthier, J.; Ghiri, E.; Gillard, J.; Gorys, V.; Poirier, M.; Rancourt, J.; Wernic, D.; Betageri, R.; Cardozo, M.; Jakes, S.; Lukas, S.; Patel, U.; Proudfoot, J.; Moss, N. Phosphotyrosine-containing dipeptides as high-affinity ligands for the p56lck SH2 domain. *J. Med. Chem.* **1999**, *42*, 722–729. (b) Beaulieu, P. L.; Cameron, D. R.; Ferland, J.-M.; Gauthier, J.; Ghiri, E.; Gillard, J.; Gorys, V.; Poirier, M.; Rancourt, J.; Wernic, D.; Llinas-Brunet, M.; Betageri, R.; Cardozo, M.; Hickey, E. R.; Ingraham, R.; Jakes, S.; Kabacell, A.; Kirrane, T.; Lukas, S.; Patel, U.; Proudfoot, J.; Sharma, R.; Tong, L.; Moss, N. Ligands for the tyrosine kinase p56lck SH2 domain: discovery of potent dipeptide derivatives with monocharged, nonhydrolyzable phosphate replacements. *J. Med. Chem.* **1999**, *42*, 1757–1766.
- (8) Liu, W.-Q.; Vidal, M.; Mathe, C.; Perigaud, C.; Garbay, C. Inhibition of the ras-dependent mitogenic pathway by phosphopeptide prodrugs with antiproliferative properties. *Bioorg. Med. Chem. Lett.* **2000**, *10*, 669–672.
- (9) (a) Wange, R. L.; Isakov, N.; Burke, T. R.; Otaka, A.; Roller, P. P.; Watts, J. D.; Aebersold, R.; Samelson, L. E. F<sub>2</sub>(PMP)<sub>2</sub>-TAM $\xi_3$ , a novel competitive inhibitor of the binding of ZAP-70 to the T cell antigen receptor, blocks early T-cell signaling. *J. Biol. Chem.* **1995**, *270*, 944–948. (b) Hall, H.; Williams, E. J.; Moore, S. E.; Walsh, F. S.; Prochiantz, A.; Doherty, P. Inhibition of FGF stimulated phosphatidylinositol hydrolysis and neurite outgrowth by a cell-membrane permeable phosphopeptide. *Curr. Biol.* **1996**, *6*, 580–587. (c) Williams, E. J.; Dunican, E. J.; Green, P. J.; Howell, F. V.; Derossi, D.; Walsh, F. S.; Doherty, P. Selective inhibition of growth factor stimulated mitogenesis by a cell-permeable Grb2-binding peptide. *J. Biol. Chem.* **1997**, *272*, 22349–22354. (d) Cody, W. L.; Doherty, A. M.; Holland, D. R.; Panek, R. L.; Lu, G. H.; Dahring, T. K.; Rose, D. R. Design of peptidomimetics that inhibit the association of phosphatidylinositol 3-kinase with platelet-derived growth factor-beta receptor and possesses cellular activity. *J. Med. Chem.* **1998**, *41*, 4329–4342.
- (10) A dimeric steroidal phosphonate derivative carrying four negative charges at physiological pH is reported to have cellular activity. Revesz, L.; Blum, E.; Manning, U.; Jachez Demange, B.; Widmer, A.; Zuber, J.-F. Non-peptide ITAM mimics as ZAP-70 antagonists. *Bioorg. Med. Chem. Lett.* **1997**, *7*, 2875–2878.
- (11) Violette, S. M.; Shakespeare, W. C.; Bartlett, C.; Guan, W.; Smith, J. A.; Rickles, R. J.; Bohacek, R. S.; Holt, D. A.; Baron, R.; Sawyer, T. K. *Chem. Biol.* **2000**, *7*, 225–235.
- (12) Wange, R. L.; Samelson, L. E. Complex Complexes: Signaling at the TCR. *Immunity* **1996**, *5*, 197–205.
- (13) (a) Lewis, L. A.; Chung, C. D.; Chen, J. I.; Parnes, J. R.; Moran, M.; Patel, V. P.; Miceli, M. C. The Lck SH2 phosphotyrosine binding site is critical for efficient TCR-induced processive tyrosine phosphorylation of the  $\zeta$ -chain and IL-2 production. *J. Immunol.* **1997**, *159*, 2292–2300. (b) Thome, M.; Germain, V.; DiSanto, J. P.; Acuto, O. The p56lck SH2 domain mediates recruitment of CD8/p56lck to the activated T cell receptor/CD3/ $\zeta$  complex. *Eur. J. Immunol.* **1996**, *26*, 2093–2100. (c) Straus, D. B.; Chan, A. C.; Patai, B.; Weiss, A. SH2 domain function is essential for the role of the Lck tyrosine kinase in T cell receptor signal transduction. *J. Biol. Chem.* **1996**, *271*, 9976–81. (d) Carrera, A. C.; Paradis, H.; Borlado, L. R.; Roberts, T. R.; Martinez, A. C. Lck unique domain influences Lck specificity and biological function. *J. Biol. Chem.* **1995**, *270*, 3385–3391.
- (14) Songyang, Z.; Shoelson, S. E.; Chaudhuri, M.; Gish, G.; Pawson, T.; Haser, W. G.; King, F.; Roberts, T.; Ratnofsky, S.; Lechleider, R. J.; Neel, B. G.; Birge, R. B.; Fajardo, J. E.; Chou, M. M.; Hanafusa, H.; Schaffhausen, B.; Cantley, L. C. SH2 Domains recognise specific phosphopeptide sequences. *Cell* **1993**, *72*, 767–778.
- (15) Tong, L.; Warren, T. C.; King, J.; Betageri, R.; Rose, J.; Jakes, S. Crystal structures of the human p56lck SH2 domain in complex with two short phosphotyrosyl peptides at 1.0 and 1.8 Å. *J. Mol. Biol.* **1996**, *256*, 601–610.
- (16) Morelock, M. M.; Ingraham, R. H.; Betageri, R.; Jakes, S. Determination of receptor–ligand kinetic and equilibrium binding constants using surface plasmon resonance: Application to the lck SH2 Domain and Phosphotyrosyl Peptides. *J. Med. Chem.* **1995**, *38*, 1309–1318.
- (17) Tong, L.; Warren, T. C.; Lukas, S.; Schembri-King, J.; Betageri, R.; Proudfoot, J.; Jakes, S. Carboxymethyl-phenylalanine as a replacement for phosphotyrosine in SH2 domain binding. *J. Biol. Chem.* **1998**, *273*, 20238–20242.
- (18) Lee, T. R.; Lawrence, D. S. Acquisition of high-affinity, SH2-targeted ligands via a spatially focused library. *J. Med. Chem.* **1999**, *42*, 784–787.
- (19) Unpublished results.
- (20) Pyridones and related heterocycles have been used in peptidomimetics against other biological targets also. See, for example: Sanderson, P. E. J.; Lyle, T. A.; Cutrona, K. J.; Dyer, D. L.; Dorsey, B. D.; McDonough, C. M.; Taylor-Olsen, A. M.; Chen, I.-W.; Chen, Z.; Cook, J. J.; Cooper, C. M.; Gardell, S. J.; Hare, T. R.; Krueger, J. A.; Lewis, S. D.; Lin, J. H.; Lucas, B. J., Jr. Efficacious, orally bioavailable thrombin inhibitors based on 3-aminopyridinone or 3-aminopyrazinone acetamide peptidomimetic templates. *J. Med. Chem.* **1998**, *41*, 4466–4474.
- (21) Luque, F. J.; Orozco, M. A new semiclassical continuum representation of solvation. *J. Phys. Chem. B.* **1997**, *101*, 5573–5582.
- (22) Miertus, S.; Scrocco, E.; Tomasi, J. Electrostatic interaction of a solute with a continuum. A direct utilization of ab initio molecular potentials for the prevision of solvent effects. *Chem. Phys.* **1981**, *55*, 117–129.
- (23) Tilley, J. W.; Danho, W.; Lovey, K.; Wagner, R.; Swistok, J.; Makofske, R.; Michalewski, J.; Triscari, J.; Nelson, D.; Weatherford, S. Carboxylic acids and tetrazoles as isosteric replacements for sulfate in cholecystokinin analogues. *J. Med. Chem.* **1991**, *34*, 1125–1136.
- (24) For details, see the Experimental Section.

- (25) Yazdanian, M.; Glynn, S. L.; Wright, J. L.; Hawi, A. Correlating partitioning and Caco-2 cell permeability of structurally diverse small molecular weight compounds. *Pharm. Res.* **1988**, *15*, 1490–1493.
- (26) Lipinski, C. A.; Lombardo, F.; Dominy, B. W.; Feeney, P. J. Experimental and computational approaches to estimate solubility and permeability in drug discovery and development settings. *Adv. Drug Delivery Rev.* **1997**, *23*, 3–25.
- (27) Conradi, R. A.; Hilgers, A. R.; Ho, N. F. H.; Burton, P. S. The influence of peptide structure on transport across caco-2 cells. II. Peptide bond modification which results in improved permeability. *Pharm. Res.* **1992**, *9*, 435–439.
- (28) Carlstrom, A.-S.; Frejd, F. Palladium catalyzed synthesis of dihydroamino acid derivatives. *Synthesis* **1989**, 414–418.
- (29) Assuming, as subsequently shown for compound **9R** and **9S**, that one enantiomer has no affinity for the SH2 domain and that all the activity resides in the active enantiomer, **7S** would have a  $K_d$  on the order of 0.6  $\mu$ M.
- (30) Assignment of absolute stereochemistry was made from a synthesis of the **9S** material starting from the chiral amino acid **IV**.
- (31) Davidson, G. A.; Varhol, R. J. Kinetics of Thapsigargin- Ca-ATPase (Sarcoplasmic Reticulum) Interaction Reveals a Two-step Binding Mechanism and Picomolar Inhibition. *J. Biol. Chem.* **1995**, *270*, 11731–11734.
- (32) These data will be published in due course (Alisa Kabcenell, manuscript in preparation).
- (33) Molecular Simulations Inc., Scranton Rd, San Diego, CA 92121-3752.
- (34) Steward, J. J. P. MOPAC Manual, MOPAC 6.0 Frank J. Seiler Research Laboratory, United State Air Force Academy, 1990.
- (35) Jorgensen, W. L.; Briggs, J. M.; Contreras, M. L. *J. Phys. Chem.* **1990**, *94*, 1683.

JM000446Q